Neural modelling to relate individual differences in physiological and perceptual responses with sensorineural hearing loss

MICHAEL G. HEINZ[1,2,*]

[1] *Department of Speech, Language, and Hearing Sciences, Purdue University, West Lafayette, IN, USA*

[2] *Weldon School of Biomedical Engineering, Purdue University, West Lafayette, IN, USA*

A great challenge in diagnosing and treating hearing impairment comes from the fact that people with similar degrees of hearing loss often have different speech-recognition abilities. Many studies of the perceptual consequences of peripheral damage have focused on outer-hair-cell (OHC) effects; however, anatomical and physiological studies suggest that many common forms of sensorineural hearing loss (SNHL) arise from mixed OHC and inner-hair-cell (IHC) dysfunction. Thus, individual differences in perceptual consequences of hearing impairment may be better explained by a more detailed understanding of differential effects of OHC/IHC dysfunction on neural coding of perceptually relevant sounds. Whereas it is difficult experimentally to estimate or control the degree of OHC/IHC dysfunction in individual subjects, computational neural models provide great potential for predicting systematically the complicated physiological effects of combined OHC/IHC dysfunction. Here, important physiological effects in auditory-nerve (AN) responses following different types of SNHL and the ability of current models to capture these effects are reviewed. In addition, a new approach is presented for computing spike-train metrics of speech-in-noise envelope coding to predict how differential physiological effects may contribute to individual differences in speech intelligibility.

INTRODUCTION

In the last 35 years, our knowledge of the physiological aspects of sensorineural hearing loss (SNHL) has expanded tremendously; however, despite these advances, very little physiological knowledge of SNHL goes into the design or fitting of hearing aids today. Although it is often difficult to relate experimentally measured physiological and perceptual findings, computational modelling provides great promise for quantitatively relating physiological and perceptual effects of SNHL in translational applications (Heinz, 2010). In fact, long before the accuracy of sensory models allowed such potential to be realized, a general theoretical framework (Fig. 1) was described for using mathematical models in the development of sensory

*Corresponding author: mheinz@purdue.edu

Proceedings of ISAAR 2015: Individual Hearing Loss – Characterization, Modelling, Compensation Strategies. 5th symposium on Auditory and Audiological Research. August 2015, Nyborg, Denmark. Edited by S. Santurette, T. Dau, J. C. Dalsgaard, L. Tranebjærg, and T. Andersen. ISBN: 978-87-990013-5-4. The Danavox Jubilee Foundation, 2015.

prostheses (Biondi, 1978; Biondi and Schmid, 1972). Fortunately, in the last 20 years advances in the complexity and accuracy of computational models of normal and impaired auditory systems have dramatically improved their potential for use in the quantitative design and fitting of hearing aids (e.g., Bondy *et al.*, 2004).

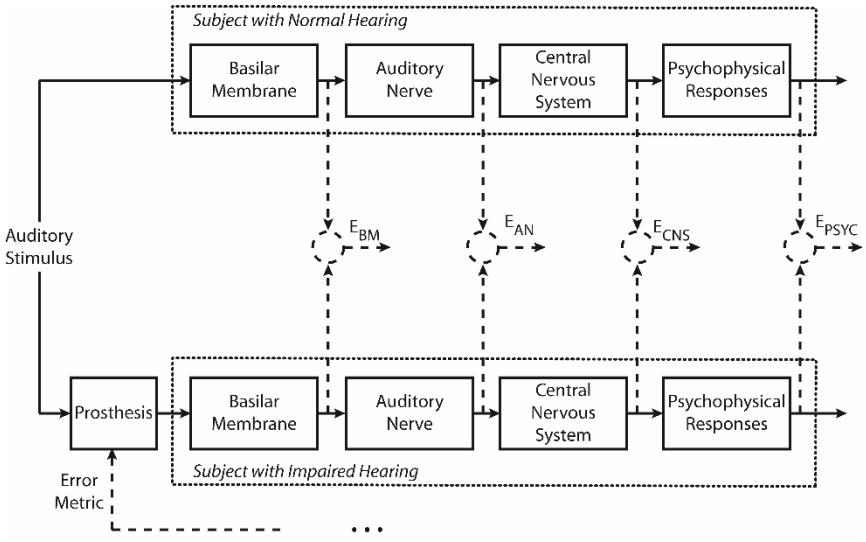

Fig. 1: Modelling framework for the design of auditory prostheses. The goal of the prosthesis is to restore normal auditory responses in a subject with impaired hearing. Computational models allow this goal to be optimally pursued by adjusting the prosthesis to minimize an error metric that quantifies the difference between normal and aided-impaired model responses. Error metrics can be derived based on models of responses at different levels of the auditory system, ranging from basilar-membrane to psychophysical responses. Modified and extended from Biondi (1978).

Current audiological diagnoses classify all types of SNHL into a single category, despite clear individual differences within this one category (e.g., different speech recognition among patients with similar audiograms). It has long been believed (and perhaps still is in some places) that mild-moderate SNHL is primarily outer-hair-cell (OHC) based (with degraded frequency selectivity responsible for difficulty understanding speech), and that inner-hair-cell (IHC) effects only play a role in cases where threshold shifts are greater than 60 dB (e.g., Edwards, 2004; Moore, 1995). In fact, much insight into perceptual effects of SNHL has been derived from considering the effects of OHC dysfunction on basilar-membrane responses (Moore, 1995; Oxenham and Bacon, 2003). However, anatomical and physiological evidence suggests that many common forms of SNHL are likely to involve mixed OHC/IHC dysfunction, and that IHC dysfunction can significantly affect perceptually relevant response properties in the auditory nerve (AN) related to intensity and speech coding. Thus, applications of computational models to account for sources of individual

physiological differences in SNHL require modelling at the AN (rather than basilar membrane).

PHYSIOLOGICAL EFFECTS OF SNHL COMMONLY DERIVE FROM A MIXTURE OF IHC AND OHC DYSFUNCTION

Liberman and Dodds (1984) established a strong correlation between AN tuning-curve shapes following cochlear damage and the status of the underlying hair cells. Hair-cell stereocilia condition provided a much stronger correlation with threshold shift than did hair-cell survival. Unlike the well-defined "tip" and "tail" region of normal AN tuning curves, significant OHC stereocilia loss produced reduced tip sensitivity and broadened tuning, whereas damage to IHC stereocilia produced threshold elevations at all frequencies with little effect on frequency selectivity. In contrast to the longstanding belief that OHC dysfunction is the primary correlate of mild-moderate SNHL, anatomical evidence from these noise-induced hearing loss studies showed major overlap in the cochlear regions with OHC and IHC stereocilia damage, and in fact often showed broader regions of IHC stereocilia damage (see Figs. 4, 5, 7, 8, and 9 in Liberman and Dodds, 1984).

In addition to noise-induced hearing loss, age-related hearing loss (or presbycusis) is also likely to include a mixture of IHC/OHC dysfunction. Schmiedt *et al.* (2002) demonstrated that young gerbils with furosemide-induced endocochlear-potential (EP) reductions showed physiological audiograms that matched those of aged gerbils (with similar reductions in EP). Furthermore, these audiograms showed the typical sloping high-frequency hearing loss characteristic of age-related hearing loss in humans. Reductions in EP have been shown to produce physiological AN responses (e.g., broadened tuning, reduced spontaneous and driven firing rates) consistent with mixed OHC/IHC dysfunction (Sewell, 1984). A mixed hair-cell loss fits with the view that the EP provides the battery that drives transduction in both types of hair cells. In summary, the available anatomical and physiological evidence suggests that many common forms of SNHL (e.g., noise and age) involve mixed OHC/IHC dysfunction.

MODEL REQUIREMENTS TO RELATE INDIVIDUAL DIFFERENCES IN PHYSIOLOGICAL AND PERCEPTUAL EFFECTS OF SNHL

The combined (and sometimes confounding) effects of OHC and IHC dysfunction in the same cochlear frequency region are likely to be quite complicated. Computational neural models provide great potential for predicting systematically the complicated physiological effects of combined OHC/IHC dysfunction. Based on anatomical and physiological knowledge of peripheral effects of SNHL, general requirements are now clear for computational modelling approaches to relate individual differences in physiological and perceptual responses with SNHL: 1) inclusion of both OHC and IHC dysfunction, since each is likely to occur in common forms of SNHL (e.g., age and noise); 2) ability to predict responses to arbitrary complex signals, since deficits often occur in complex listening situations (e.g., speech in noise); 3) accurate representation of temporal responses (both rapid and slow), since both timescales are likely to be perceptually relevant in many tasks for which listeners with SNHL have

particular difficulty (e.g., source segregation, speech intelligibility in real-world background noises); 4) ability to evaluate cochlear synaptopathy, since a reduction in the number of IHC synapses occurs with age and moderate noise exposure, even in cases without permanent threshold shift (Kujawa and Liberman, 2015); and 5) ability to relate spike-time responses to perceptually relevant metrics, since responses at the level of the AN are required to capture the known physiological SNHL effects.

Computational models now exist that incorporate the salient response properties (both rate and timing) that are important for modelling individual differences in OHC/IHC dysfunction (reviewed by Heinz, 2010), and numerous modelling frameworks exist for relating physiological and perceptual responses (e.g., Elhilali *et al.*, 2003; Heinz *et al.*, 2001; Hines and Harte, 2012). This chapter will focus on a well-established AN model (Bruce *et al.*, 2003; Carney, 1993; Zilany *et al.*, 2009; 2014) to review how various physiological effects of OHC/IHC dysfunction can be accounted for in computational models. This model accounts for a wide range of response properties measured from both normal and hearing-impaired animals for a wide range of stimuli (e.g., tones, noise, and speech). The model takes as input an arbitrary acoustic waveform and produces an output of spike times for a single AN fibre with a specified characteristic frequency (CF) (see Fig. 2 in Zilany *et al.*, 2009). The model allows independent control of OHC and IHC function through two parameters, C_{OHC} and C_{IHC}, ranging from 1 (normal) to 0 (fully dysfunctional).

Modelling OHC dysfunction

Damage to OHCs has been shown to result in numerous correlated effects: increased thresholds (reduced cochlear gain at CF), broadened tuning, reduced cochlear compression, reduced two-tone suppression, and reduced level dependence in phase responses. Each of these properties is believed to be associated with a single mechanism (sometimes called the cochlear amplifier), for which OHCs play a major role. Thus, a key insight into modelling the effects of OHC dysfunction is to include a single signal-processing mechanism that accounts for all of these effects together (Carney, 1993; Kates, 1991; Patuzzi, 1996), and for which the effects of OHC dysfunction can be included in a single-parameter fashion (Bruce *et al.*, 2003; for review, see Heinz, 2010). By modelling OHC dysfunction as a single parameter that controls the maximum cochlear gain at low sound levels, partial OHC damage reduces each of these nonlinear properties by an amount that is proportional to the fractional reduction in cochlear gain (see Fig. 4 in Bruce *et al.*, 2003). While insight can be gained from simpler models that isolate some of these effects, such models are limited in their generality for complex stimuli, which are likely to be critical for SNHL model applications such as hearing-aid design.

Modelling IHC dysfunction

IHC damage has often been thought of primarily in terms of complete IHC loss (i.e., dead regions); however, it is clear that dysfunction of remaining IHCs can have significant effects on perceptually relevant neural responses. Although moderate IHC dysfunction does not significantly affect tuning, there are other consistent effects on

AN response properties following IHC damage, including elevated thresholds, reduction in spontaneous and driven rates, and reduction in the slopes of rate-level functions (Liberman and Dodds, 1984; Liberman and Kiang, 1984; Wang *et al.*, 1997). It is typically believed that AN rate-level functions are steeper following SNHL, consistent with the effects of loudness recruitment; however, this has been shown not to be a consistent effect (Harrison, 1981; Heinz and Young, 2004; see Fig. 2A). IHC dysfunction was hypothesized to be responsible for reducing the rate of response growth based on one of two mechanisms. The first is that damage to IHC stereocilia may reduce the number of transduction channels that can open, resulting in a reduced maximum transduction current and a reduced response-growth slope. Second, if OHC function remains normal, IHC damage may elevate thresholds enough so that the AN-fibre rate-level function is made shallower by remaining BM compression. Thus, IHC damage can confound the effects of OHC damage on basic response properties, such as response growth with level (Fig. 2B).

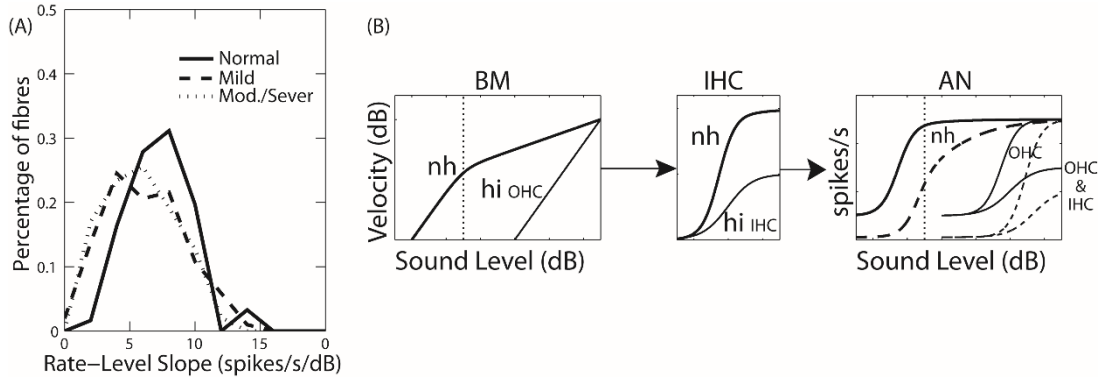

Fig. 2: (A) CF-tone AN rate-level functions were shallower than normal following noise-induced hearing loss. (B) Damage to the IHC transducer can produce shallower AN response growth despite steeper BM responses due to OHC damage. Modified from Heinz and Young (2004), Heinz *et al.* (2005).

IHC dysfunction was modelled by Bruce *et al.* (2003) with a shallower input/output transduction function, under the control of C_{IHC}. The IHC module with SNHL accounted for the wide range of rate-level functions observed experimentally (Heinz and Young, 2004; see Fig. 6 in Zilany and Bruce, 2006), and contributed to reduced synchrony capture in vowel responses (Bruce *et al.*, 2003; Miller *et al.*, 1997).

Further insight into the effects of IHC dysfunction comes from studies in chinchillas, where the platinum-based chemotherapy drug carboplatin specifically affects IHCs while leaving OHCs intact. While dose-dependent IHC loss is observed along the cochlea following carboplatin, structural damage has also been observed (e.g., to stereocilia) in remaining IHCs (Wake *et al.*, 1994), with reduced spontaneous and

driven discharge rates despite normal tuning (Wang *et al.*, 1997). Although remaining AN fibres show normal temporal coding to modulated tones (quantified by average vector strength), fewer spikes in response to sound alters the response statistics and degrades predicted detection/discriminability when both response mean and variance are considered (i.e., in terms of a *d'* metric; Axe and Heinz, 2015). Thus, reduced spike rates from IHC dysfunction may be perceptually relevant due to reduced information from less reliable responses.

Challenges in modelling mixed hair-cell dysfunction

While this signal-processing filter-bank model approach allows for implementation of an IHC transduction function that accounts for the observed range of rate-level shapes (Zilany and Bruce, 2006), it does not currently account for the reduction in spontaneous rate observed with carboplatin toxicity, noise induced hearing loss, and metabolic age-related hearing loss. Because this reduced spike count may be perceptually relevant, this is likely to be an important component to include in future models of IHC dysfunction. Also, the current independent control of OHC/IHC dysfunction does not capture directly the effects of metabolic hearing losses associated with presbycusis (Schmiedt *et al.*, 2002), where OHC and IHC function are both dependent on the same EP "battery". More biophysically based models with EP control of both OHC and IHC function have been shown to capture the main effects of metabolic presbycusis in a more physiologically constrained approach (Saremi and Stenfelt, 2013), but this is not currently possible with the phenomenological signal-processing model approach of Zilany *et al.* (2009).

COMPUTING PERCEPTUAL METRICS FROM SPIKE-TIME RESPONSES

The influence of inherent fluctuations on speech intelligibility: SNR_{ENV}

Recent psychophysically based modelling has demonstrated that the signal-to-noise ratio (SNR_{ENV}) at the output of a modulation filter bank provides a robust measure of speech intelligibility (Jørgensen and Dau, 2011). The effect of the noise (N) on speech (S) coding is assumed to: 1) reduce envelope power of S+N by filling in the dips of clean speech, and 2) introduce a noise floor due to intrinsic fluctuations in the noise itself. Changes in the SNR_{ENV} metric with acoustic processing/distortion can be related to a change in speech reception threshold (SRT). An ideal-observer framework is used to convert SNR_{ENV} to percent correct. The central hypothesis of this modelling framework is that the predicted change in intelligibility arises because the processing (or in this case SNHL) changes the input (acoustic) SNR needed to obtain the SNR_{ENV} corresponding to a given percent correct. SNR_{ENV} predicted speech intelligibility across a wider range of degraded conditions than many long-standing speech-intelligibility models (e.g., STI). Key insight into the effect of spectral subtraction on speech intelligibility was garnered by consideration of the modulation-domain SNR, which factors in the inherent fluctuations within the noise. Although spectral subtraction increased the envelope power in the noisy-speech (leading STI-based metrics to predict improvements), it also increased the envelope power in the noise-

alone response to a greater degree such that SNR_{ENV} decreased, consistent with the observed performance degradation.

Extending the envelope power spectrum model (SNR_{ENV}) to neural responses

While the promise of the SNR_{ENV} metric has been demonstrated for normal-hearing listeners (Jørgensen and Dau, 2011), it has yet to be thoroughly extended to hearing-impaired listeners because of limitations in our physiological knowledge of how SNHL affects the envelope coding of speech in noise relative to noise alone. Here, envelope coding to non-periodic stimuli (e.g., speech in noise) was quantified from model neural spike trains using shuffled-correlogram analyses, which were analysed in the modulation frequency domain to compute modulation-band based estimates of signal and noise envelope coding (e.g., a neural SNR_{ENV} metric).

Neural spike-train responses were obtained from the most recent version of the AN model (Zilany *et al.*, 2014), with responses from medium-spontaneous-rate fibres considered here. Figure 3 shows the single sentence considered in this initial study, along with predicted AN-fibre discharge rate waveforms for a CF=1 kHz fibre to clean speech, noisy speech, and noise alone. The noise used was broadband Gaussian noise, spectrally matched to the sentence. Strong speech modulations are seen in the clean-speech response, with only the largest and slowest modulations apparent in the noisy-speech response. Inherent fluctuations in the noise-alone response are seen, which are an important factor in the envelope power spectrum model analyses (Jørgensen and Dau, 2011). Shuffled correlogram analyses were used to quantify envelope coding in each condition (Louage *et al.*, 2004; Swaminathan and Heinz, 2011). By averaging correlograms from positive- and negative-polarity versions of each stimulus, the *sumcor* (Fig. 3B top) quantifies the temporal envelope coding in terms of an autocorrelation function, whereas the Fourier transform of the sumcor estimates the envelope power-spectral density (Fig. 3B bottom). As in the envelope power spectrum model analyses, the SNR_{ENV} metric was computed for each fibre CF and modulation filter band by computing the ratio of the response envelope power for speech (estimated as the envelope power to noisy speech (S+N) minus the envelope power to noise alone) divided by the envelope power to noise alone (see Eqs. 2 and 4 in Jørgensen and Dau, 2011). Here, envelope power was computed within seven modulation-frequency bands (Fig. 3C) by integrating the envelope power spectral density within different modulation-frequency ranges (a low-pass range at and below 1 Hz, and six octave-spaced bands centred at 2 to 64 Hz with a bandwidth equal to the centre frequency, i.e., Q=1). Although not implemented directly as modulation filters, these seven modulation bands correspond closely to the seven original modulation bands (Jørgensen and Dau, 2011). A total SNR_{ENV} (see Fig. 4) was computed by combining the individual SNR_{ENV} values from each modulation band and each acoustic filter (as in Eq. 6 of Jørgensen and Dau, 2011). In this initial study, four AN-fibre CFs were used (0.5, 1, 2, and 4 kHz) to compute SNR_{ENV} as a function of acoustic SNR (Fig. 4) for several versions of the AN model (normal hearing, 30-dB OHC loss, and mixed 15-dB/15-dB IHC/OHC loss). For SNHL model versions, a speech level of 80 dB SPL was used so that all comparisons were at equal sensation level (SL).

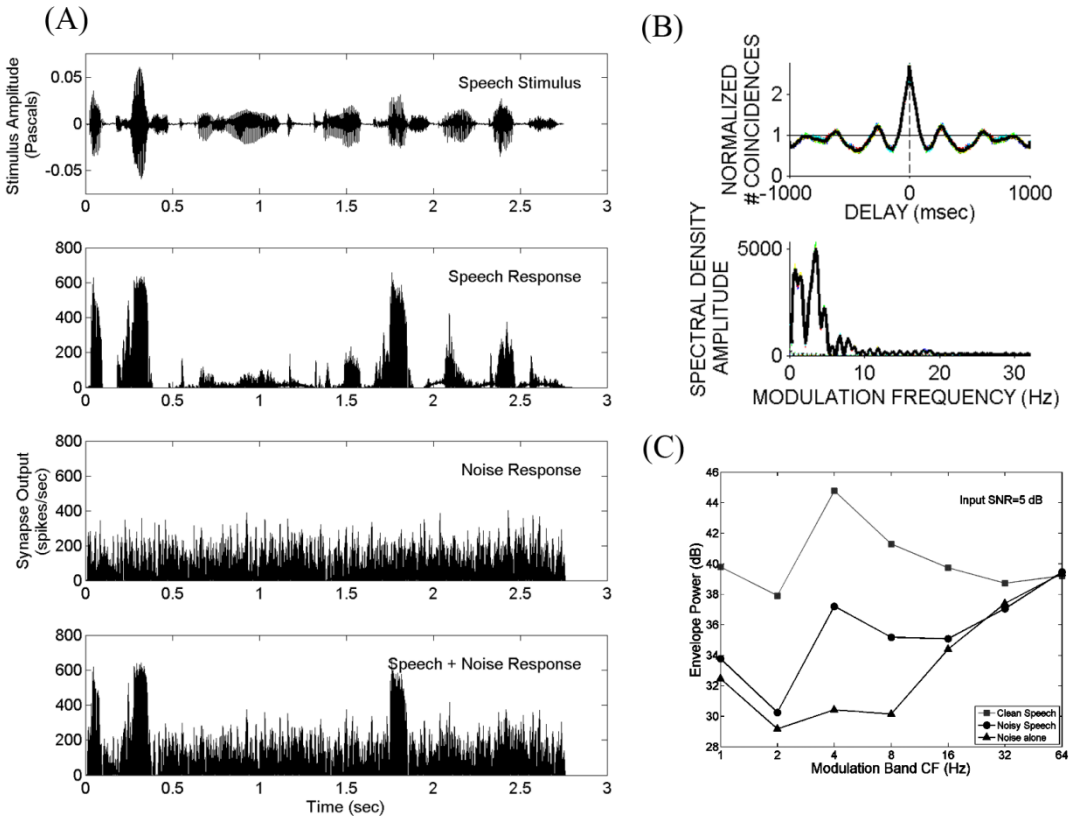

Fig. 3: Extending the envelope power spectrum model analysis of SNR_{ENV} (Jørgensen and Dau, 2011) to neural spike-train responses. (A) One speech sentence with overall sound level of 50 dB SPL (best modulation level for this fibre; top row) was presented to a medium-spontaneous-rate model AN fibre with CF = 1 kHz (2nd row). Noise-alone (3rd row) and noisy-speech responses (bottom row) are shown for a 5-dB acoustic SNR condition. (B) The shuffled-correlogram *sumcor* (top) was used to quantify temporal envelope coding in each response, with the *envelope power spectral density* estimated as the Fourier transform of the sumcor (bottom). (C) Envelope power as a function of modulation-band centre frequency computed from the envelope spectral density for clean speech, noisy speech, and noise alone.

Preliminary predictions of the effect of individual differences on SNR_{ENV}

Overall, many aspects of the SNR_{ENV} predictions computed here from neural spike trains showed close similarities to the psychoacoustical model predictions motivating this work (Jørgensen and Dau, 2011). 1) Envelope power excitation patterns (e.g., Figs. 3C and 5) showed the same relative position across conditions, with the highest envelope power for clean speech, the lowest envelope power for noise alone, and noisy speech in between. 2) The peak in speech envelope power was observed in the

4-Hz modulation band. 3) Negligible differences were predicted between noisy-speech and noise-alone envelope power (i.e., zero SNR_{ENV}) for the 16-64 Hz modulation bands. 4) The total SNR_{ENV} varied from about 2 dB to 14 dB as acoustic (input) SNR varied from −9 to 9 dB, with these neural values being above the neural noise floor in all conditions.

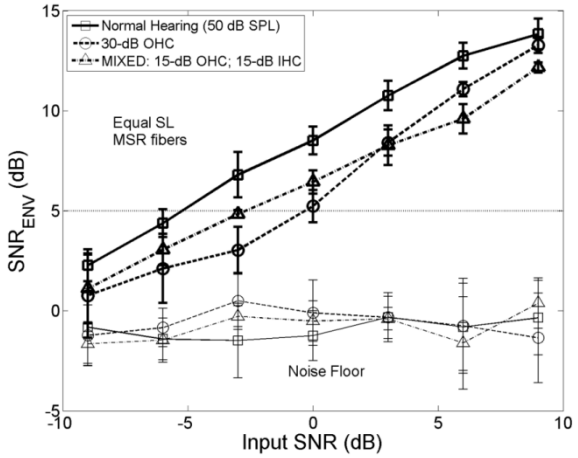

Fig. 4: Individual differences in speech intelligibility are predicted with varying degrees of OHC/IHC dysfunction. Neural-based predictions of total SNR_{ENV} are shown as a function of input (acoustic) SNR for three versions of the AN model that varied in OHC/IHC dysfunction. All comparisons were made at equal SL, using medium-spontaneous-rate (MSR) fibres. A neural noise floor is shown based on randomized spike times.

Predictions of total SNR_{ENV} as a function of acoustic SNR (Fig. 4) varied across the three AN-model versions with different degrees of OHC/IHC dysfunction. Both SNHL versions predicted reduced SNR_{ENV} relative to normal hearing, with a ~5-dB acoustic (input) SNR loss (estimated at SNR_{ENV} = 5 dB) for 30-dB OHC dysfunction and ~2.5-dB SNR loss for 30-dB mixed OHC/IHC dysfunction. A cross-over between OHC and mixed predictions was observed at 3-dB input SNR, with OHC dysfunction predictions nearly matching normal hearing at the highest SNR. The cross-over is due to a greater SNR loss (rightward shift) in the OHC function for low SNRs (e.g., more noise through broad filters) and less SNR loss for cleaner speech.

This spike-train approach allows the exploration of individual differences in the modulation domain for noisy-speech encoding. For these 30-dB hearing losses and equal-SL comparisons, there was (Fig. 5): 1) less difference across model versions for clean speech, 2) reduced envelope power for noisy speech, 3) reduced (but less so than noisy speech) envelope power for noise alone (intrinsic fluctuations), 4) resulting overall reductions in SNR_{ENV} (from 2nd and 3rd points), and 5) differences predicted when IHC dysfunction (i.e., shallower transduction) was included.

SUMMARY AND IMPLICATIONS

Modelling at the AN level is required to include the physiological factors known to influence neural coding of complex sounds: 1) OHC dysfunction, 2) IHC dysfunction, 3) IHC loss (dead regions), 4) EP reduction in presbycusis, 5) cochlear synaptopathy. Preliminary spike-train analyses show strong similarities to the speech envelope power spectrum model of Jørgensen and Dau (2011), which has shown the importance of SNR_{ENV} for predicting speech intelligibility across a wide range of processing conditions. While these preliminary neural predictions are shown here primarily to demonstrate the feasibility of neural SNR_{ENV} computations from spike-train responses, the cross-over in Fig. 4 suggests that individual differences may occur based on differential degrees of OHC/IHC dysfunction in listeners currently diagnosed into the single category of SNHL. These neural computations will be applied in future animal studies to quantify the effects of various types of SNHL on coding of speech and inherent noise modulations, which may provide valuable insight for understanding individual differences in speech-in-noise intelligibility.

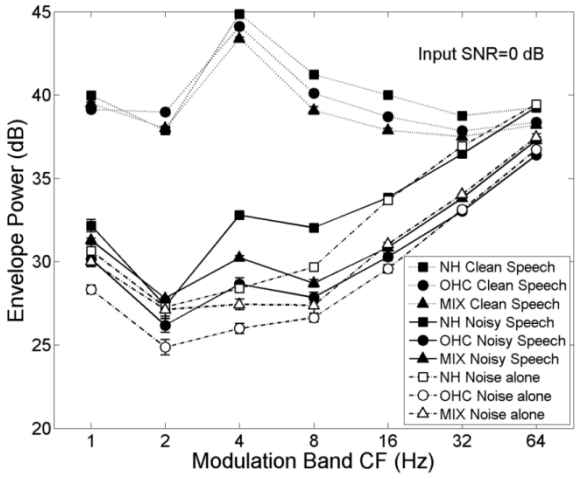

Fig. 5: Envelope power as a function of modulation-band centre frequency for clean-speech, noisy-speech, and noise-alone responses from AN-model versions that varied in OHC/IHC dysfunction (as in Fig. 4).

ACKNOWLEDGMENTS

Varsha Rallapalli assisted with the neural SNR_{ENV} computations. Søren Jørgensen, Torsten Dau, and Christoph Scheidiger are thanked for discussions on the speech envelope power spectrum model. This work was supported by an NIH grant (R01-DC009838) and an International Project Grant from Action on Hearing Loss.

REFERENCES

Axe, D.R. and Heinz, M.G. (**2015**). "The effects of carboplatin-induced ototoxicity on temporal coding in the auditory nerve," Assoc. Res. Otolaryngol. Abstr., **38**, 76-77.

Biondi, E. and Schmid, R. (**1972**). "Mathematical models and prostheses for sense organs," in *Theory and Applications of Variable Structure Systems*. Eds. R.R. Mohler and A. Ruberti (Academic Press, London), pp. 183-211.

Biondi, E. (**1978**). "Auditory processing of speech and its implications with respect to prosthetic rehabilitation. The bioengineering viewpoint," Audiology, **17**, 43-50.

Bondy, J., Becker, S., Bruce, I.C., Trainor, L., and Haykin, S. (**2004**). "A novel signal-processing strategy for hearing-aid design: Neurocompensation," Signal Process., **84**, 1239-1253.

Bruce, I.C., Sachs, M.B., and Young, E.D. (**2003**). "An auditory-periphery model of the effects of acoustic trauma on auditory nerve responses," J. Acoust. Soc. Am., **113**, 369-388.

Carney, L.H. (**1993**). "A model for the responses of low-frequency auditory-nerve fibers in cat," J. Acoust. Soc. Am., **93**, 401-417.

Edwards, B. (**2004**). "Hearing aids and hearing impairment," in *Speech Processing in the Auditory System*. Ed. S. Greenberg, W.A. Ainsworth, A.N. Popper, and R.R. Fay (Springer, New York), pp. 339-421.

Elhilali, M., Chi, T., and Shamma, S.A. (**2003**). "A spectro-temporal modulation index (STMI) for assessment of speech intelligibility," Speech Commun., **41**, 331-348.

Harrison, R.V. (**1981**). "Rate-versus-intensity functions and related AP responses in normal and pathological guinea pig and human cochleas," J. Acoust. Soc. Am., **70**, 1036-1044.

Heinz, M.G., Colburn, H.S., and Carney, L.H. (**2001**). "Evaluating auditory performance limits: I One-parameter discrimination using a computational model for the auditory nerve," Neural Comput., **13**, 2273-2316.

Heinz, M.G. and Young, E.D. (**2004**). "Response growth with sound level in auditory-nerve fibers after noise-induced hearing loss," J. Neurophysiol., **91**, 784-795.

Heinz, M.G., Issa, J.B., and Young, E.D. (**2005**). "Auditory-nerve rate responses are inconsistent with common hypotheses for the neural correlates of loudness recruitment," J. Assoc. Res. Otolaryngol., **6**, 91-105.

Heinz, M.G. (**2010**). "Computational Modeling of Sensorineural Hearing Loss," in *Computational Models of the Auditory System*, Eds. R. Meddis, E.A. Lopez-Poveda, A.N. Popper, and R.R. Fay (Springer, New York), pp. 177-202.

Hines, A. and Harte, N. (**2012**). "Speech intelligibility prediction using a Neurogram Similarity Index Measure," Speech Commun., **54**, 306-320.

Jørgensen, S. and Dau, T. (**2011**). "Predicting speech intelligibility based on the signal-to-noise envelope power ratio after modulation-frequency selective processing," J. Acoust. Soc. Am., **130**, 1475-1487.

Kates, J.M. (**1991**). "A time-domain digital cochlear model," IEEE Trans. Signal Process., **39**, 2573-2592.

Kujawa, S.G. and Liberman, M.C. (**2015**). "Synaptopathy in the noise-exposed and aging cochlea: Primary neural degeneration in acquired sensorineural hearing loss," Hear. Res., **330**, 191-199.

Liberman, M.C. and Dodds, L.W. (**1984**). "Single-neuron labeling and chronic cochlear pathology III Stereocilia damage and alterations of threshold tuning curves," Hear. Res., **16**, 55-74.

Liberman, M.C. and Kiang, N.Y.S. (**1984**). "Single-neuron labeling and chronic cochlear pathology IV Stereocilia damage and alterations in rate- and phase-level functions," Hear. Res., **16**, 75-90.

Louage, D.H., van der Heijden, M., and Joris, P.X. (**2004**). "Temporal properties of responses to broadband noise in the auditory nerve," J. Neurophysiol., **91**, 2051-2065.

Miller, R.L., Schilling, J.R., Franck, K.R., and Young, E.D. (**1997**). "Effects of acoustic trauma on the representation of the vowel /ε/ in cat auditory nerve fibers," J. Acoust. Soc. Am., **101**, 3602-3616.

Moore, B.C.J. (**1995**). *Perceptual Consequences of Cochlear Damage* (Oxford University Press, New York).

Oxenham, A.J. and Bacon, S.P. (**2003**). "Cochlear compression: Perceptual measures and implications for normal and impaired hearing," Ear Hearing, **24**, 352-366.

Patuzzi, R. (**1996**). "Cochlear micromechanics and macromechanics," in *The Cochlea*. Eds. P. Dallos, A.N. Popper, and R.R. Fay (Springer, New York), pp. 186-257.

Saremi, A. and Stenfelt, S. (**2013**). "Effect of metabolic presbyacusis on cochlear responses: A simulation approach using a physiologically-based model," J. Acoust. Soc. Am., **134**, 2833-2851.

Schmiedt, R.A., Lang, H., Okamura, H.O., and Schulte, B.A. (**2002**). "Effects of furosemide applied chronically to the round window: A model of metabolic presbyacusis," J. Neurosci., **22**, 9643-9650.

Sewell, W.F. (**1984**). "The effects of furosemide on the endocochlear potential and auditory-nerve fiber tuning curves in cats," Hear. Res., **14**, 305-314.

Swaminathan, J. and Heinz, M.G. (**2011**). "Predicted effects of sensorineural hearing loss on across-fiber envelope coding in the auditory nerve," J. Acoust. Soc. Am., **129**, 4001-4013.

Wake, M., Takeno, S., Ibrahim, D., and Harrison, R. (**1994**). "Selective inner hair cell ototoxicity induced by carboplatin," Laryngoscope, **104**, 488-493.

Wang, J., Powers, N., Hofstetter, P., Trautwein, P., Ding, D., and Salvi, R. (**1997**). "Effects of selective inner hair cell loss on auditory nerve fiber threshold, tuning and spontaneous and driven discharge rate," Hear. Res., **107**, 67-82.

Zilany, M.S.A. and Bruce, I.C. (**2006**). "Modeling auditory-nerve responses for high sound pressure levels in the normal and impaired auditory periphery," J. Acoust. Soc. Am., **120**, 1446-1466.

Zilany, M.S.A., Bruce, I.C., Nelson, P.C., and Carney, L.H. (**2009**). "A phenomenological model of the synapse between the inner hair cell and auditory nerve: Long-term adaptation with power-law dynamics," J. Acoust. Soc. Am., **126**, 2390-2412.

Zilany, M.S.A., Bruce, I.C., and Carney, L.H. (**2014**). "Updated parameters and expanded simulation options for a model of the auditory periphery," J. Acoust. Soc. Am., **135**, 283-286.